JACS
JOURNAL OF THE AMERICAN CHEMICAL SOCIETY
Article
pubs.acs.org/JACS

Molecular Imaging of Peroxynitrite with HKGreen-4 in Live Cells and Tissues

Tao Peng,[†,‡] Nai-Kei Wong,[†,‡] Xingmiao Chen,[⊥] Yee-Kwan Chan,[§] Derek Hoi-Hang Ho,[†] Zhenning Sun,[†] Jun Jacob Hu,[†] Jiangang Shen,[⊥] Hani El-Nezami,[§] and Dan Yang*[,†]

[†]Morningside Laboratory for Chemical Biology and Department of Chemistry, [⊥]School of Chinese Medicine, and [§]School of Biological Sciences, The University of Hong Kong, Pokfulam Road, Hong Kong, P. R. China

Supporting Information

ABSTRACT: Peroxynitrite ($ONOO^-$), the product of a radical combination reaction of nitric oxide and superoxide, is a potent biological oxidant involved in a broad spectrum of physiological and pathological processes. Herein we report the development, characterization, and biological applications of a new fluorescent probe, HKGreen-4, for peroxynitrite detection and imaging. HKGreen-4 utilizes a peroxynitrite-triggered oxidative *N*-dearylation reaction to achieve an exceptionally sensitive and selective fluorescence turn-on response toward peroxynitrite in chemical systems and biological samples. We have thoroughly evaluated the utility of HKGreen-4 for intracellular peroxynitrite imaging and, more importantly, demonstrated that HKGreen-4 can be efficiently employed to visualize endogenous peroxynitrite generated in *Escherichia coli*-challenged macrophages and in live tissues from a mouse model of atherosclerosis. This probe should serve as a powerful molecular imaging tool to explore peroxynitrite biology under a variety of physiological and pathological contexts.

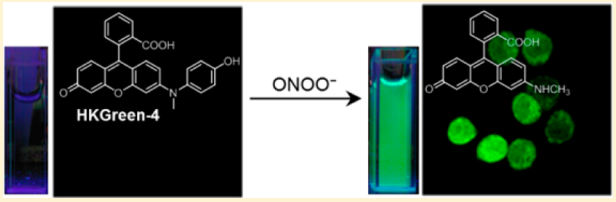

INTRODUCTION

Peroxynitrite ($ONOO^-$), the diffusion-controlled reaction product of nitric oxide ($^{\bullet}NO$) and superoxide ($O_2^{\bullet-}$), has been considered a "stealthy" biological oxidant by virtue of its elusive nature and multiple *in vivo* reaction targets.[1] Being a strong oxidant and good nucleophile, $ONOO^-$ can react with different biomolecules, including proteins, transition-metal-containing enzyme centers, lipids, and nucleic acids, through direct oxidation or decomposing into highly reactive secondary radicals such as hydroxyl radical ($^{\bullet}OH$), carbonate radical ($CO_3^{\bullet-}$), and nitrogen dioxide ($^{\bullet}NO_2$), eventually contributing to cell death. Therefore, $ONOO^-$ is widely assumed to account for most of the cytotoxicity previously ascribed to $^{\bullet}NO$ and $O_2^{\bullet-}$ and has been implicated in a growing list of diseases, such as cardiovascular and neurodegenerative disorders, metabolic diseases, inflammation, pain, and cancer.[2] Meanwhile, $ONOO^-$ is also reported to display protective activities *in vivo* by functioning as a cytotoxic effector against invading pathogens and as a signaling molecule.[1,3] For instance, $ONOO^-$ generated from activated macrophages has been suggested to mediate intracellular killing of invading *Escherichia coli*,[4] *Rhodococcus equi*,[5] and *Trypanosoma cruzi*.[6] Recent evidence indicates that $ONOO^-$ also plays underappreciated roles in the redox regulation of key signaling pathways that are dependent on tyrosine phosphorylation via its ability to selectively nitrate tyrosine residues.[3] However, most of the beneficial effects of $ONOO^-$ *in vivo* remain controversial or poorly characterized,[7] probably due to a lack of reliable methods for unambiguously monitoring $ONOO^-$ levels *in vivo*.[2c]

Historically, most of the studies about biological $ONOO^-$ formation rely on its footprint reaction, i.e., nitration of tyrosine residues to form 3-nitrotyrosines, which, however, cannot be used as unique evidence for $ONOO^-$ formation because of the existence of other nitrating species *in vivo* and for real-time $ONOO^-$ detection.[8] To better define the physiological and pathological roles of $ONOO^-$ *in vivo*, there has been a strong demand for reliable analytical methods with high spatiotemporal resolution for $ONOO^-$ detection. Indeed, fluorescent probes, featuring high sensitivity and real-time spatial imaging capacity, have been accorded great importance in the detection of reactive oxygen species (ROS), reactive nitrogen species (RNS), and reactive sulfur species (RSS).[9] During the past several years, we and other groups have reported a number of small-molecule and protein-based fluorescent probes for $ONOO^-$ detection,[10] some of which have found utility in biological studies.[11] Nevertheless, it remains challenging to design probes that can be robustly employed in diverse biological systems, especially in living mammalian tissues. Moreover, the elusive nature of $ONOO^-$, stemming from its extremely short half-life (i.e., ~10 ms), low steady-state concentration (i.e., nM range),[2b] and complex chemistry amidst various potentially interfering ROS and RNS in cellular milieu, naturally calls for highly sensitive and selective probes for its direct and unambiguous detection.

Herein we report the design and characterization of HKGreen-4, a new small-molecule turn-on fluorescent probe

Received: May 8, 2014
Published: July 24, 2014

dx.doi.org/10.1021/ja504624q | J. Am. Chem. Soc. 2014, 136, 11728−11734

for exceptionally sensitive and selective detection of $ONOO^-$ in aqueous solution, live cells, and tissues. HKGreen-4 exploits an *N*-phenylrhodol-based fluorescence "off–on" switch and an $ONOO^-$-triggered oxidative *N*-dearylation reaction to achieve a robust fluorescence turn-on response toward peroxynitrite over a range of biologically relevant ROS/RNS. We demonstrate the versatile utility of HKGreen-4 in biological contexts by showing that this probe can be used for intracellular $ONOO^-$ imaging in a variety of cell types by both single-photon and two-photon excitation fluorescence microscopy. Moreover, we show that HKGreen-4 can be employed to visualize the kinetics of $ONOO^-$ generation in macrophages challenged with heat-killed *E. coli* and prove that the $ONOO^-$ generation is enzymatically regulated. Furthermore, the probe can also be utilized to image the endogenous peroxynitrite generation in live tissues from a mouse model of atherosclerosis.

RESULTS AND DISCUSSION

Design and Synthesis of Probes. The reaction-based approach for developing selective fluorescent probes in biological systems represents a new research focus that has attracted increasing attention.[9d] Previously, our group discovered that $ONOO^-$ can selectively react with a trifluoromethyl ketone moiety through direct nucleophilic addition to form a dioxirane intermediate, which can then oxidize a nearby anisole ring to a dienone compound with concomitant C–O bond cleavage of the anisole.[10b,12] On the basis of this nucleophilic reaction between $ONOO^-$ and trifluoromethyl ketone, we have developed several reaction-based small-molecule fluorescent probes for $ONOO^-$ detection.[10b,c,f] Notably, integration of this $ONOO^-$-selective reaction into an *N*-phenylrhodol fluorescence "off–on" switch (Scheme 1) afforded a rhodol-based fluorescent probe, HKGreen-3, for $ONOO^-$ detection.[10f,13] Apart from its nucleophilicity, $ONOO^-$ also exhibits potent oxidizing capability, allowing for direct oxidation of electron-rich groups through one- or two-electron oxidation processes.[2a] As highly electron-rich phenol and aniline derivatives could be easily oxidized by $ONOO^-$, we expect that incorporation of simple phenol and anilines into the *N*-phenylrhodol scaffold would afford novel reaction-based probes for $ONOO^-$ detection. Therefore, we designed a new series of molecules, **1**–**5**, bearing simple electron-donating substituents, such as methoxyl, hydroxyl, and amino groups, on the phenyl ring of *N*-phenyl-*N*-methylrhodol (Scheme 1). Upon reaction with $ONOO^-$, these molecules could readily undergo oxidative *N*-dearylation to release strongly fluorescent *N*-methylrhodol.[10f] Although previous work by Nagano's group showed that an analogous *O*-dearylation reaction can be used to develop fluorescent probes, i.e., HPF and APF, for detection of highly reactive oxygen species (hROS),[14] those probes cannot differentiate $ONOO^-$ from other interfering ROS/RNS. We expect that the *N*-phenylrhodol scaffold would be uniquely advantageous, as the rhodol fluorescence is highly efficiently quenched by the *N*-phenyl group.[13] More importantly, the nitrogen atom of rhodol could further increase the electron density of the *N*-phenyl ring, resulting in high reactivity toward $ONOO^-$ over other ROS/RNS. Compounds **1**–**5** were synthesized according to our previously developed synthetic route to rhodol fluorophores (Schemes S2 and S3, Supporting Information).[13,15]

Scheme 1. Design of a New Series of Rhodol-Based Compounds for Detecting Peroxynitrite

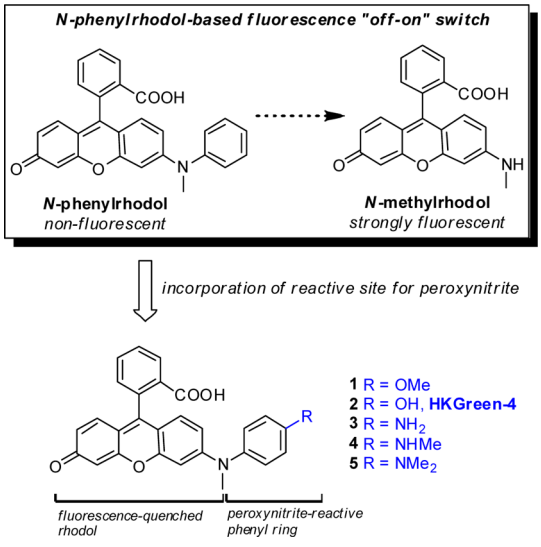

Screening Probes for Peroxynitrite Detection. With compounds **1**–**5** in hand, we first examined their reactivity toward $ONOO^-$ and hypochlorous acid (HOCl), a potentially interfering hROS in $ONOO^-$ detection, in aqueous solutions buffered at physiological pH (0.1 M phosphate buffer, pH 7.4). As expected, most of these compounds, except compound **1**, exhibited strong fluorescence increases upon treatment with $ONOO^-$, while displaying differential fluorescence responses toward HOCl (Figures S1 and S2, Supporting Information). Notably, compound **2** with a hydroxy substituent responded to $ONOO^-$ much more dramatically than toward HOCl (Figures S1 and S2). On the other hand, compounds **3**–**5** with various amino substituents generally gave stronger fluorescence responses toward HOCl than toward $ONOO^-$ when the oxidants were present in excess amounts (Figure S2). We propose that $ONOO^-$ oxidizes compounds **2**–**5** through direct two-electron oxidation of the electron-rich phenyl rings to form iminium ions,[16] which are further hydrolyzed to give the *N*-dearylation product (Schemes S6). By contrast, HOCl reacts with compounds **2**–**5** through *N*-chlorination,[17] which ultimately leads to *N*-dearylation (Schemes S6). Due to steric hindrance of the diarylamine moiety and competition with chlorination at the phenol *ortho* positions (Schemes S6),[18] *N*-chlorination of compound **2** with HOCl is much slower and less efficient than oxidation by $ONOO^-$, thereby resulting in efficient distinction of $ONOO^-$ from HOCl. Detailed mechanistic studies on the *N*-dearylation reactions of those compounds induced by $ONOO^-$ and HOCl are currently underway.

As the phenol compound **2**, called HKGreen-4 hereafter (Scheme 2), can differentiate $ONOO^-$ from HOCl and exhibits high sensitivity toward $ONOO^-$, we focused our subsequent

Scheme 2. *N*-Dearylation Reaction of HKGreen-4 Induced by Peroxynitrite for Its Fluorescence Detection

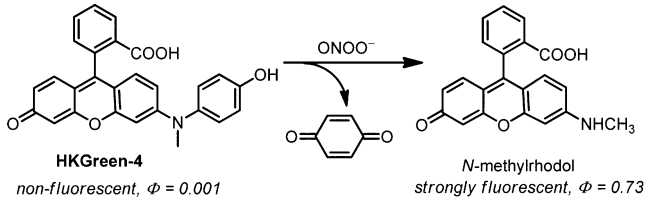

dx.doi.org/10.1021/ja504624q | J. Am. Chem. Soc. 2014, 136, 11728–11734

studies on this probe for detailed characterization in both chemical and biological systems.

Reactivity and Selectivity of HKGreen-4 for Peroxynitrite. Spectroscopic properties of HKGreen-4 were evaluated in aqueous solution buffered at physiological pH (0.1 M phosphate buffer, pH 7.4). HKGreen-4 exhibited a strong absorption peak at 517 nm in the UV spectrum (Figure S3), suggesting that the probe exists predominately as the "open" quinoid form in aqueous solution.[19] As expected, HKGreen-4 was virtually non-fluorescent in aqueous solution (Φ = 0.001; Figures 1A and S3), owing to effective fluorescence quenching of the rhodol core fluorophore by the *N*-phenyl group.[13] Addition of $ONOO^-$ to a solution of HKGreen-4 (1 μM in phosphate buffer, pH 7.4) resulted in a dramatic and rapid fluorescence turn-on response with maximal emission at 535 nm in a dose-dependent manner (Figure 1A). In less than 5 s (Figure S4) after addition of 1 equiv of $ONOO^-$ into HKGreen-4 solution, a 290-fold fluorescence increase was observed, much higher than the responses of our previous-generation fluorescent probes for $ONOO^-$. A linear relationship was observed between fluorescence intensity and $ONOO^-$ concentration up to 1 equiv of $ONOO^-$ (Figure S5). Fluorescence intensity then reached a plateau on further addition of $ONOO^-$ up to 4 equiv (Figure S6). The detection limit of HKGreen-4 for $ONOO^-$ was estimated to be as low as 10 nM, at which a 3-fold fluorescence increase could be achieved. HPLC and LC-MS analysis confirmed that the fluorescent product was indeed *N*-methylrhodol (Φ = 0.73; Scheme 2 and Figure S10), resulting from the $ONOO^-$-induced *N*-dearylation reaction of HKGreen-4.

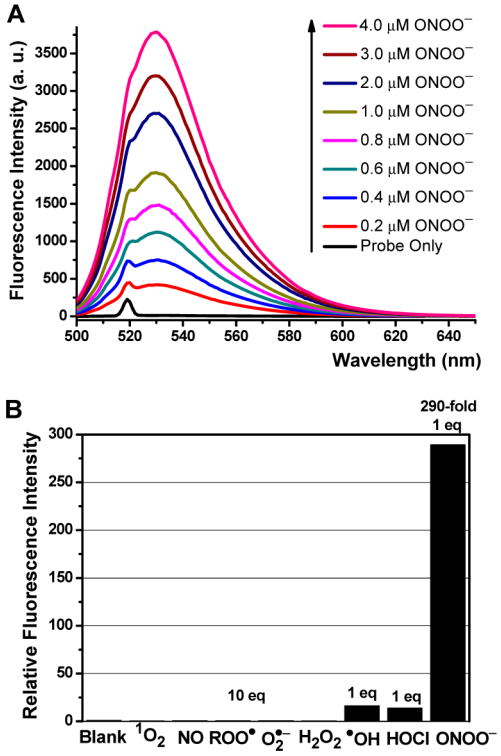

Figure 1. (A) Fluorescence response of 1 μM HKGreen-4 to different amounts of $ONOO^-$. (B) Relative fluorescence intensity (λ_{em} = 535 nm) of 1 μM HKGreen-4 toward various ROS and RNS. Data were acquired at 25 °C in 0.1 M phosphate buffer at pH 7.4, with excitation at 517 nm. ROS and RNS were slowly added to HKGreen-4 solution with vigorously stirring. Reactions were then carried out for 30 min at room temperature before the fluorescence intensity of the probe solution was measured.

Reactivity of HKGreen-4 toward a panel of ROS and RNS was tested to establish the selectivity of the probe for detecting $ONOO^-$ (Figure 1B). While most of the biologically relevant ROS and RNS, including H_2O_2, $^1O_2$, $^\bullet NO$, $O_2^{\bullet-}$, and $ROO^\bullet$, even when presented as 10 equiv, did not trigger any fluorescence increases of the probe, potentially interfering hROS, such as HOCl and $^\bullet OH$, induced much weaker and nearly negligible fluorescence increases, i.e., >18-fold lower increases, compared to $ONOO^-$. Together, these results suggest that HKGreen-4 outperforms previously reported probes for $ONOO^-$ detection in terms of lower working concentration, greater fluorescence response, and better selectivity over HOCl and $^\bullet OH$.

To further evaluate HKGreen-4 for $ONOO^-$ detection in chemical systems, we proceeded to perform additional experiments. The probe exhibited efficient fluorescence turn-on response to $ONOO^-$ within a biologically relevant pH range from 6.5 to 9.5 (Figure S7). Moreover, HKGreen-4 still showed comparable fluorescence increase toward $ONOO^-$ in the presence of CO_2 (Figure S8), which is ubiquitous in biological systems and reacts with $ONOO^-$ through nucleophilic addition at a high rate constant.[1] Addition of DMSO (i.e., 0.1% v/v, ~14 mM) as an effective $^\bullet OH$ scavenger[20] into the probe solution did not attenuate the fluorescence response of HKGreen-4 to $ONOO^-$ (Figure S9), indicating that $^\bullet OH$, one of the secondary decomposition radicals of $ONOO^-$, does not contribute to the fluorescence increase of HKGreen-4 in the presence of $ONOO^-$. By contrast, DMSO can completely

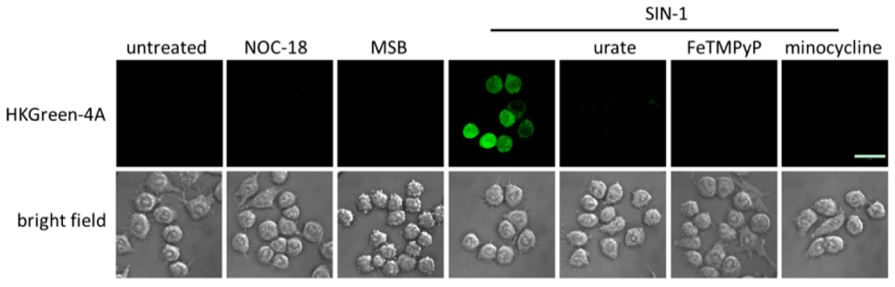

Figure 2. Validation of HKGreen-4 selectivity with exogenous ROS/RNS donors in RAW264.7 macrophages. Cells were coincubated with HKGreen-4A (10 μM) and donors for $^\bullet NO$, $O_2^{\bullet-}$, or $ONOO^-$ for 1 h, followed by confocal fluorescence imaging. NOC-18 (500 μM), MSB (100 μM), and SIN-1 (50 μM) were used for producing $^\bullet NO$, $O_2^{\bullet-}$, and $ONOO^-$, respectively. Urate (100 μM)/minocycline (100 μM) and FeTMPyP (50 μM) are $ONOO^-$ scavengers and decomposition catalyst, respectively. Scale bar represents 20 μm.

dx.doi.org/10.1021/ja504624q | J. Am. Chem. Soc. 2014, 136, 11728−11734

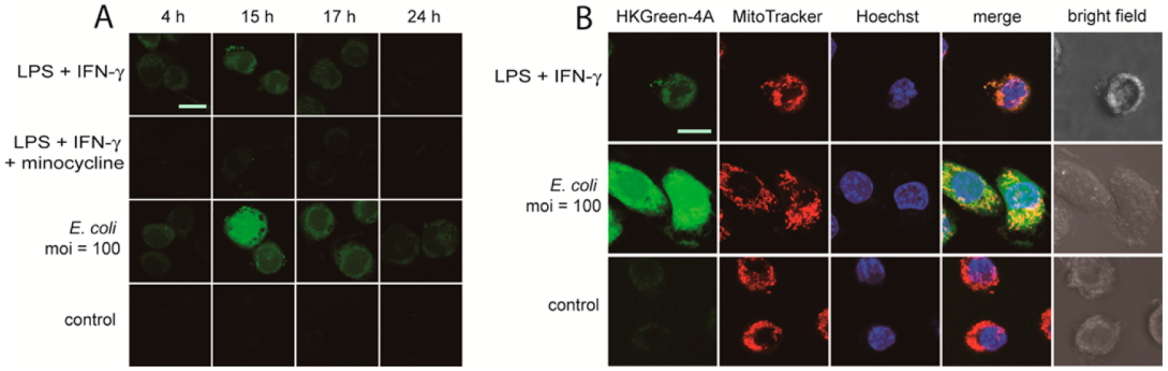

Figure 3. Confocal fluorescence imaging of endogenous $ONOO^-$ with HKGreen-4 in stimulated RAW264.7 macrophages. (A) Kinetics of $ONOO^-$ generation upon stimulation with LPS (1 μg/mL) and IFN-γ (100 ng/mL), or heat-killed *E. coli* (multiplicity of infection (moi) = 100) for the indicated time. $ONOO^-$ was detected by staining cells with HKGreen-4A (10 μM; 30 min) before confocal imaging. Minocycline (100 μM) was added to scavenge $ONOO^-$. (B) Cells were treated for 14 h with LPS/IFN-γ, or heat-killed *E. coli*, and then stained (30 min) with HKGreen-4A (10 μM), MitoTracker Red (100 nM), and Hoechst 33342 (75 ng/mL) before confocal imaging. Scale bars represent 10 μm.

suppress the fluorescence increases of HKGreen-4 and compound **3** induced by HOCl (Figure S9), suggesting that HOCl can readily oxidize DMSO[21] even before it reacts with the probes and that using DMSO as a co-solvent (i.e., 0.1% v/v) for making HKGreen-4 solution can minimize the interference from HOCl in $ONOO^-$ detection. These results collectively indicate that HKGreen-4 can robustly detect $ONOO^-$ in aqueous solution.

Evaluation of HKGreen-4 for Imaging Peroxynitrite in Live Cells. We then examined the potential of HKGreen-4 to visualize $ONOO^-$ in live cells by confocal fluorescence microscopy. In order to improve the intracellular loading of HKGreen-4, we prepared its acetate derivative, HKGreen-4A (Scheme S5), which has superior cell membrane permeability,[10f,22] and used it in all subsequent cell imaging experiments. Several exogenous ROS and RNS donors were employed to validate the selectivity of HKGreen-4 in live cells. As shown in Figure 2, mouse RAW264.7 macrophages loaded with HKGreen-4 showed barely detectable background fluorescence. A significant increase in intracellular fluorescence was observed in cells treated with 3-morpholinosydnonimine hydrochloride (SIN-1), an $ONOO^-$ generator, but not in cells treated with 3,3-bis(aminoethyl)-1-hydroxy-2-oxo-1-triazene (NOC-18, an NO donor) or menadione sodium bisulfite (MSB, an $O_2^{\bullet-}$ donor) (Figure 2). Fluorescence increase in SIN-1-treated cells was significantly attenuated in the presence of $ONOO^-$ scavengers, such as urate and minocycline,[23] or FeTMPyP, an $ONOO^-$ decomposition catalyst.[1]

We also established that HKGreen-4 can be robustly applied in other cells types, such as C17.2 mouse neural progenitor cells, CHO (Chinese hamster ovarian) cells, and BV-2 mouse microglia, to imaging SIN-1 generated $ONOO^-$ (Figure S12). Moreover, the cytotoxicity of HKGreen-4A was assessed by MTT assay in RAW264.7 cells (Figure S11), which indicated that this probe is virtually nontoxic to cells even at 80 μM after 24 h incubation. Taken together, these results confirmed that HKGreen-4 is well-suited for selective intracellular imaging of $ONOO^-$ in live biological samples.

Visualization of Endogenous Peroxynitrite Production in Macrophages under Immune Stimulation. Next, we focused on assessing the performance of HKGreen-4 in imaging endogenous $ONOO^-$ in RAW264.7 mouse macrophages, which are known to produce $ONOO^-$ upon stimulation with bacterial endotoxin lipopolysaccharide (LPS; *Salmonella typhimurium*), pro-inflammatory cytokine interferon-gamma (IFN-γ), and phorbol 12-myristate 13-acetate (PMA).[10c,f] It has been suggested that $ONOO^-$ generated in macrophages may contribute to the bactericidal activity of these cells.[4b,c,5] We therefore sought to use HKGreen-4 to examine whether $ONOO^-$ is produced in macrophages when challenged with heat-killed *E. coli*, a model bacterial species. First, a kinetic analysis of $ONOO^-$ production in activated RAW264.7 macrophages was performed. Briefly, cells were challenged with a combination of LPS and IFN-γ, or heat-killed *E. coli* for different durations (t = 4, 15, 17, and 24 h), and incubated with HKGreen-4A for 30 min before confocal imaging. Due to much higher sensitivity of HKGreen-4 than our previously reported $ONOO^-$ probes, a lower probe working concentration, i.e., 10 μM, of HKGreen-4A was needed to achieve optimal fluorescence signals.[10c,f] In contrast to previously used stimulation conditions of macrophages with LPS, IFN-γ, and PMA,[10c,f] we omitted the usage of PMA throughout our studies, as PMA is a plant toxin and irrelevant to the bacterial infection model we are interested in. As shown in Figure 3A, upon LPS/IFN-γ or *E. coli* stimulation, HKGreen-4 gave a strong fluorescence increase in activated RAW264.7 cells in a time-dependent manner, with detectable fluorescence signals at 4 h and maximal signals being observed between 15 and 17 h post-treatment, followed by a discernible decline, suggesting that $ONOO^-$ production in macrophages is temporally controlled, in a manner consistent with the temporally regulated generation of its precursor $^{\bullet}NO$ in stimulated macrophages.[24]

Having optimized the $ONOO^-$ induction time in macrophages, we proceeded to evaluate the intracellular localization of HKGreen-4 in activated macrophages by confocal microscopy. Co-staining experiments with MitoTracker Red and HKGreen-4A in LPS/IFN-γ-stimulated macrophages revealed broad spatial overlap of these two probes (Figure 3B), indicating that under low and moderate stimulation conditions (i.e., LPS/IFN-γ stimulation) mitochondria might be the major source for $O_2^{\bullet-}$, and therefore for $ONOO^-$. In contrast, with strong stimulants like heat-killed *E. coli*, macrophages exhibited maximum and broadly diffused green fluorescence encompassing both nuclear and cytoplasmic compartments, suggesting that HKGreen-4 and its fluorescent product diffuse freely inside the cells and that under these conditions mitochondria might not be the only source of $O_2^{\bullet-}$ and $ONOO^-$.

dx.doi.org/10.1021/ja504624q | J. Am. Chem. Soc. 2014, 136, 11728−11734

To expand the utility of HKGreen-4 for cellular imaging studies, we also demonstrated that HKGreen-4 can be utilized to visualize endogenous $ONOO^-$ production in primary mouse macrophages that were differentiated with M-CSF from mouse bone marrow progenitor cells and stimulated with LPS (*E. coli* K12) for 18 h (Figure S13). Moreover, HKGreen-4 can be applied to two-photon excitation microscopy (λ_{ex} = 730 nm, λ_{em} = 500−550 nm) for peroxynitrite imaging in stimulated macrophages (Figure S14), further establishing the versatile applicability of HKGreen-4 for molecular imaging studies.

Next, we used HKGreen-4 to validate whether $ONOO^-$ formation in *E. coli*-challenged macrophages is enzymatically regulated, which would provide important insights into the biological functions of $ONOO^-$. It has been controversial that regulated $ONOO^-$ formation can be temporally achieved in stimulated macrophages, as the generations of $O_2^{\bullet-}$ from NADPH oxidase (NOX) and $^{\bullet}NO$ from inducible nitric oxide synthase (iNOS) seem temporally divergent.[25] HKGreen-4 should serve as a unique tool to address this controversy. To this end, imaging studies of *E. coli*-challenged macrophages using HKGreen-4 were performed in the presence of well-established inhibitors for NOX and iNOS to assess $ONOO^-$ formation. MitoSOX Red was used in parallel for monitoring $O_2^{\bullet-}$ throughout our studies. As shown in Figure 4, strong

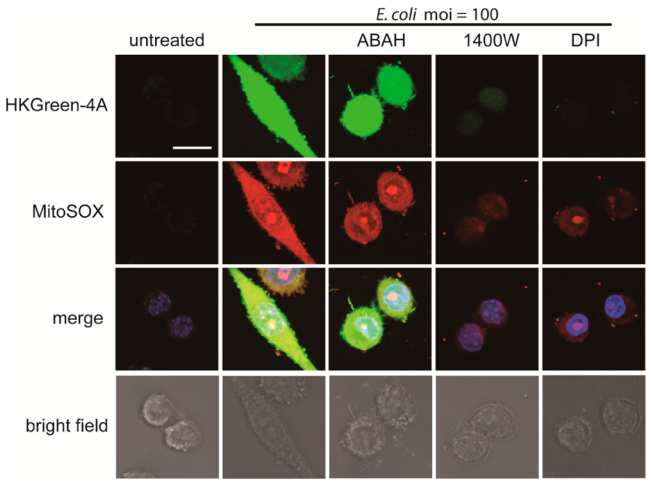

Figure 4. Pharmacological validation of enzymatic pathways involved in endogenous $ONOO^-$ formation in *E. coli*-challenged RAW264.7 macrophages. Cells were cotreated with heat-killed *E. coli* (moi = 100) and various enzyme inhibitors for 14 h, and then stained with HKGreen-4A (10 μM), MitoSOX (2.5 μM), and Hoechst 33342 (75 ng/mL) for 30 min before confocal imaging. ABAH (50 μM) is an inhibitor of myeloperoxidase that produces HOCl. 1400W (100 nM) and DPI (50 nM) are inhibitors for iNOS and NOX, respectively. "Merge" represents overlay of all fluorescence channels including Hoechst. Scale bar represents 10 μm.

intracellular fluorescence signals from HKGreen-4 and MitoSOX Red were observed in *E. coli*-challenged macrophages at 14 h post-treatment. Conventional scavengers for $ONOO^-$, $O_2^{\bullet-}$, and $^{\bullet}NO$, i.e., urate, TEMPOL, and cPTIO, respectively, can effectively suppress the green fluorescence signal of HKGreen-4 (Figure S15). In addition, 4-aminobenzoic acid hydrazide (ABAH), a potent inhibitor for myeloperoxidase (MPO) that catalyzes the generation of HOCl, did not affect fluorescence increase of HKGreen-4 (Figure 4). These results further confirm the generation of $ONOO^-$ in *E. coli*-challenged macrophages. On the other hand, 1400W and aminoguanidine (AG), as a selective iNOS inhibitor and a nonselective NOS inhibitor, respectively, both effectively abolished $ONOO^-$ formation in *E. coli*-challenged macrophages (Figures 4 and S15). Interestingly, 1400W also evidently reduced MitoSOX Red fluorescence (Figure 4), consistent with recent observations that 1400W, in addition to inhibiting iNOS activity, also attenuates $O_2^{\bullet-}$ production *in vivo*.[26] Moreover, well-documented NOX inhibitors, such as dibenziodolium chloride (DPI) and apocynin, also greatly attenuated $ONOO^-$ generation (Figures 4 and S15). Taken together, our cell imaging experiments using HKGreen-4 provide the direct visualization evidence that $ONOO^-$ is indeed generated in *E. coli*-challenged macrophages, likely as an immune effector for bacterial clearance, and suggest that $ONOO^-$ formation in *E. coli*-challenged macrophages is enzymatically regulated and dependent on iNOS-generated NO and NOX-derived $O_2^{\bullet-}$.

Imaging Peroxynitrite in Live Tissues from a Mouse Model of Atherosclerosis. Finally, we sought to apply HKGreen-4 to image $ONOO^-$ in live tissue samples. $ONOO^-$ formation has long been implicated in the pathogenesis of atherosclerosis on the basis of indirect detection, i.e., immunostaining of protein nitration, which, however, cannot be used as unique evidence for $ONOO^-$ formation.[8] To the best of our knowledge, direct evidence about abnormal $ONOO^-$ formation under atherosclerosis conditions is still lacking.[2a,27] To address this question, we employed an apolipoprotein E knockout ($ApoE^{-/-}$) mouse model that readily develops atherosclerosis on a normal chow diet. Wild-type C57BL/6 and $ApoE^{-/-}$ mice (n = 6 per group) were fed a normal chow diet for 20 weeks before sacrifice. Under anesthesia, living heart tissues were perfused with HKGreen-4A (2 μM) in Hank's balanced salt solution (HBSS) for 30 min, followed by fixation and quenching with 4% PFA and glycine, respectively. Mouse hearts were then excised and cryosectioned at 10 μm intervals to reveal the aortic roots for confocal imaging under two-photon excitation settings. As shown in Figure 5, an obvious fluorescence increase, i.e., about 2-fold, from HKGreen-4 was observed at the smooth muscle of the aortic root from $ApoE^{-/-}$ mice compared to the samples from wild-type mice (Figure S16). This result indicates that HKGreen-4 is well-retained during histological sample preparation and sensitive enough to visualize endogenous $ONOO^-$ in live tissues. More importantly, our study also provides the first direct evidence linking elevated $ONOO^-$ formation with atherosclerotic conditions.

■ CONCLUSION

In summary, we have presented the development, chemical characterization, and molecular imaging applications of a new fluorescent probe, HKGreen-4, for $ONOO^-$ detection in aqueous solution, live cells, and tissues. HKGreen-4 contains a rhodol core fluorophore and a peroxynitrite-triggered fluorescence "off−on" switch that afford excellent sensitivity and selectivity in fluorescence detection of $ONOO^-$ over other biologically relevant ROS and RNS with visible excitation and green emission profiles. We have thoroughly demonstrated that HKGreen-4 can be utilized to image cellular $ONOO^-$ in various cell types with minimal cytotoxicity by both single-photon and two-photon excitation microscopy. Live cell imaging with HKGreen-4 revealed that $ONOO^-$ formation in activated macrophages is temporally and enzymatically regulated, and may potentially be an important effector in immune response. Moreover, HKGreen-4 can also be

dx.doi.org/10.1021/ja504624q | J. Am. Chem. Soc. 2014, 136, 11728−11734

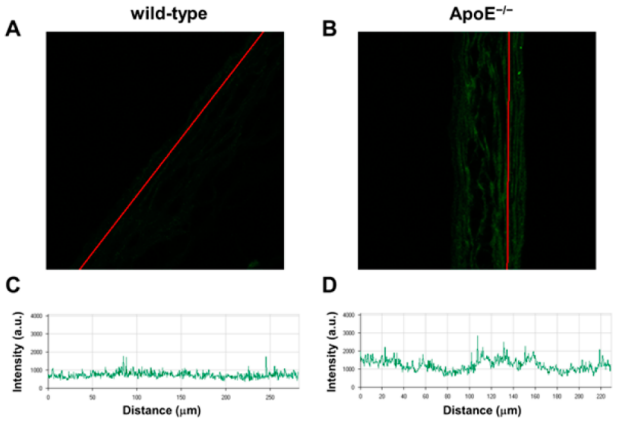

Figure 5. Tissue staining of endogenous $ONOO^-$ with HKGreen-4 in mouse heart smooth muscles. Living smooth muscles of the mouse aortic root were stained with HKGreen-4A (2 μM) for 30 min by perfusion, fixed, cryosectioned, and mounted for two-photon confocal imaging. (A) Transverse section of wild-type smooth muscles. (B) Transverse section of $ApoE^{-/-}$ smooth muscles. (C) Profile of fluorescence intensity of region of interest in (A). (D) Profile of fluorescence intensity of region of interest in (B). Fluorescence images were generated by merging 20 photosections from z-stack imaging and are representative of HKGreen-4 staining of each group (n = 6 mice) in two independent experiments. More representative images are included in Figure S16 in Supporting Information.

employed for live tissue staining, which confirmed that $ONOO^-$ is generated at elevated levels in a mouse model of atherosclerosis. Collectively, HKGreen-4 has been established with practical utility and represents a robust molecular imaging tool for unraveling the physiological and pathological consequences of $ONOO^-$ formation under a variety of biological contexts.

■ ASSOCIATED CONTENT

Ⓢ Supporting Information

Experimental details for chemical synthesis of all compounds, supplementary photophysical characterization of all probes, and imaging methods and data. This material is available free of charge via the Internet at http://pubs.acs.org.

■ AUTHOR INFORMATION

Corresponding Author

yangdan@hku.hk

Author Contributions

‡T.P. and N.-K.W. contributed equally.

Notes

The authors declare the following competing financial interest(s): D.Y. and T.P. hold patents on HKGreen-4 and HKGreen-4A.

■ ACKNOWLEDGMENTS

This work was supported by The University of Hong Kong, the University Development Fund, Hong Kong Research Grants Council (HKU 706410, 776512M, and 777611M), and Morningside Foundation. We thank Dr. Aimin Xu at Department of Pharmacology and Pharmacy, The University of Hong Kong, for kindly providing the $ApoE^{-/-}$ mouse model, Dr. Jing Guo for technical assistance, and Faculty Core Facility of the Li Ka Shing Faculty of Medicine at HKU for confocal microscopy.

■ REFERENCES

(1) Radi, R. *J. Biol. Chem.* **2013**, *288*, 26464.
(2) (a) Pacher, P.; Beckman, J. S.; Liaudet, L. *Physiol. Rev.* **2007**, *87*, 315. (b) Szabo, C.; Ischiropoulos, H.; Radi, R. *Nat. Rev. Drug Discovery* **2007**, *6*, 662. (c) Ferrer-Sueta, G.; Radi, R. *ACS Chem. Biol.* **2009**, *4*, 161.
(3) Liaudet, L.; Vassalli, G.; Pacher, P. *Front Biosci.* **2009**, *14*, 4809.
(4) (a) Zhu, L.; Gunn, C.; Beckman, J. S. *Arch. Biochem. Biophys.* **1992**, *298*, 452. (b) Xia, Y.; Zweier, J. L. *Proc. Natl. Acad. Sci. U.S.A.* **1997**, *94*, 6954. (c) Allen, R. G.; Lafuse, W. P.; Powell, N. D.; Webster Marketon, J. I.; Stiner-Jones, L. T. M.; Sheridan, J. F.; Bailey, M. T. *Infect. Immun.* **2012**, *80*, 3429.
(5) Darrah, P. A.; Hondalus, M. K.; Chen, Q.; Ischiropoulos, H.; Mosser, D. M. *Infect. Immun.* **2000**, *68*, 3587.
(6) (a) Denicola, A.; Rubbo, H.; Rodriguez, D.; Radi, R. *Arch. Biochem. Biophys.* **1993**, *304*, 279. (b) Alvarez, M. N.; Peluffo, G.; Piacenza, L.; Radi, R. *J. Biol. Chem.* **2011**, *286*, 6627.
(7) Fang, F. C. *Nat. Rev. Microbiol.* **2004**, *2*, 820.
(8) (a) Oury, T. D.; Tatro, L.; Ghio, A. J.; Piantadosi, C. A. *Free Radic. Res.* **1995**, *23*, 537. (b) Singh, R. J.; Goss, S. P. A.; Joseph, J.; Kalyanaraman, B. *Proc. Natl. Acad. Sci. U.S.A.* **1998**, *95*, 12912. (c) Hurst, J. K. *J. Clin. Invest.* **2002**, *109*, 1287.
(9) (a) Wardman, P. *Free Radic. Biol. Med.* **2007**, *43*, 995. (b) McQuade, L. E.; Lippard, S. J. *Curr. Opin. Chem. Biol.* **2010**, *14*, 43. (c) Chen, X.; Tian, X.; Shin, I.; Yoon, J. *Chem. Soc. Rev.* **2011**, *40*, 4783. (d) Chan, J.; Dodani, S. C.; Chang, C. J. *Nat. Chem.* **2012**, *4*, 973. (e) Lippert, A. R.; Van de Bittner, G. C.; Chang, C. J. *Acc. Chem. Res.* **2011**, *44*, 793. (f) Yang, Y.; Zhao, Q.; Feng, W.; Li, F. *Chem. Rev.* **2012**, *113*, 192. (g) Li, X.; Gao, X.; Shi, W.; Ma, H. *Chem. Rev.* **2014**, *114*, 590. (h) Simen Zhao, B.; Liang, Y.; Song, Y.; Zheng, C.; Hao, Z.; Chen, P. R. *J. Am. Chem. Soc.* **2010**, *132*, 17065. (i) Zhao, B. S.; Zhang, G.; Zeng, S.; He, C.; Chen, P. R. *Integr. Biol.* **2013**, *5*, 1485. (j) Pu, K.; Shuhendler, A. J.; Rao, J. *Angew. Chem., Int. Ed.* **2013**, *52*, 10325. (k) Shuhendler, A. J.; Pu, K.; Cui, L.; Uetrecht, J. P.; Rao, J. *Nat. Biotechnol.* **2014**, *32*, 373. (l) Lippert, A. R.; New, E. J.; Chang, C. J. *J. Am. Chem. Soc.* **2011**, *133*, 10078. (m) Qian, Y.; Karpus, J.; Kabil, O.; Zhang, S.-Y.; Zhu, H.-L.; Banerjee, R.; Zhao, J.; He, C. *Nat. Commun.* **2011**, *2*, 495. (n) Liu, C.; Pan, J.; Li, S.; Zhao, Y.; Wu, L. Y.; Berkman, C. E.; Whorton, A. R.; Xian, M. *Angew. Chem., Int. Ed.* **2011**, *50*, 10327. (o) Peng, B.; Chen, W.; Liu, C.; Rosser, E. W.; Pacheco, A.; Zhao, Y.; Aguilar, H. C.; Xian, M. *Chem.—Eur. J.* **2014**, *20*, 1010. (p) Lin, V. S.; Lippert, A. R.; Chang, C. J. *Proc. Natl. Acad. Sci. U.S.A.* **2013**, *110*, 7131. (q) Peng, H.; Cheng, Y.; Dai, C.; King, A. L.; Predmore, B. L.; Lefer, D. J.; Wang, B. *Angew. Chem., Int. Ed.* **2011**, *50*, 9672. (r) Sasakura, K.; Hanaoka, K.; Shibuya, N.; Mikami, Y.; Kimura, Y.; Komatsu, T.; Ueno, T.; Terai, T.; Kimura, H.; Nagano, T. *J. Am. Chem. Soc.* **2011**, *133*, 18003. (s) Xuan, W.; Sheng, C.; Cao, Y.; He, W.; Wang, W. *Angew. Chem., Int. Ed.* **2012**, *51*, 2282. (t) Lin, V. S.; Chang, C. J. *Curr. Opin. Chem. Biol.* **2012**, *16*, 595.
(10) (a) Ueno, T.; Urano, Y.; Kojima, H.; Nagano, T. *J. Am. Chem. Soc.* **2006**, *128*, 10640. (b) Yang, D.; Wang, H.-L.; Sun, Z.-N.; Chung, N.-W.; Shen, J.-G. *J. Am. Chem. Soc.* **2006**, *128*, 6004. (c) Sun, Z.-N.; Wang, H.-L.; Liu, F.-Q.; Chen, Y.; Tam, P. K. H.; Yang, D. *Org. Lett.* **2009**, *11*, 1887. (d) Sikora, A.; Zielonka, J.; Lopez, M.; Joseph, J.; Kalyanaraman, B. *Free Radic. Biol. Med.* **2009**, *47*, 1401. (e) Yang, D.; Sun, Z.-N.; Peng, T.; Wang, H.-L.; Shen, J.-G.; Chen, Y.; Tam, P. K.-H. In *Live Cell Imaging: Methods and Protocols*; Papkovsky, D. B., Ed.; Humana Press: New York, 2009; Vol. *591*, p 93. (f) Peng, T.; Yang, D. *Org. Lett.* **2010**, *12*, 4932. (g) Zielonka, J.; Sikora, A.; Joseph, J.; Kalyanaraman, B. *J. Biol. Chem.* **2010**, *285*, 14210. (h) Xu, K.; Chen, H.; Tian, J.; Ding, B.; Xie, Y.; Qiang, M.; Tang, B. *Chem. Commun.* **2011**, *47*, 9468. (i) Tian, J.; Chen, H.; Zhuo, L.; Xie, Y.; Li, N.; Tang, B. *Chem.—Eur. J.* **2011**, *17*, 6626. (j) Yu, F.; Li, P.; Li, G.; Zhao, G.; Chu, T.; Han, K. *J. Am. Chem. Soc.* **2011**, *133*, 11030. (k) Zhang, Q.; Zhu, Z.; Zheng, Y.; Cheng, J.; Zhang, N.; Long, Y.-T.; Zheng, J.; Qian, X.; Yang, Y. *J. Am. Chem. Soc.* **2012**, *134*, 18479. (l) Lin, K.-K.; Wu, S.-C.; Hsu, K.-M.; Hung, C.-H.; Liaw, W.-F.; Wang, Y.-M. *Org. Lett.* **2013**, *15*, 4242. (m) Yu, F.; Li, P.; Wang, B.; Han, K. *J. Am. Chem. Soc.*

2013, *135*, 7674. (n) Chen, Z.-J.; Ren, W.; Wright, Q. E.; Ai, H.-W. *J. Am. Chem. Soc.* **2013**, *135*, 14940.
(11) (a) Gaupels, F.; Spiazzi-Vandelle, E.; Yang, D.; Delledonne, M. *Nitric Oxide* **2011**, *25*, 222. (b) Ieda, N.; Nakagawa, H.; Horinouchi, T.; Peng, T.; Yang, D.; Tsumoto, H.; Suzuki, T.; Fukuhara, K.; Miyata, N. *Chem. Commun.* **2011**, *47*, 6449. (c) Ieda, N.; Nakagawa, H.; Peng, T.; Yang, D.; Suzuki, T.; Miyata, N. *J. Am. Chem. Soc.* **2012**, *134*, 2563. (d) Ling, T.; Vandelle, E.; Bellin, D.; Kleinfelder-Fontanesi, K.; Huang, J. J.; Chen, A. M. D. J.; Delledonne, M. *Nitric Oxide* **2012**, *27* (Suppl.), S9. (e) Serrano, I.; Romero-Puertas, M. C.; Rodríguez-Serrano, M.; Sandalio, L. M.; Olmedilla, A. *J. Exp. Bot.* **2012**, *63*, 1479.
(12) (a) Yang, D.; Tang, Y.-C.; Chen, J.; Wang, X.-C.; Bartberger, M. D.; Houk, K. N.; Olson, L. *J. Am. Chem. Soc.* **1999**, *121*, 11976. (b) Yang, D.; Wong, M.-K.; Yan, Z. *J. Org. Chem.* **2000**, *65*, 4179.
(13) Peng, T.; Yang, D. *Org. Lett.* **2010**, *12*, 496.
(14) (a) Setsukinai, K.-I.; Urano, Y.; Kikuchi, K.; Higuchi, T.; Nagano, T. *J. Chem. Soc., Perkin Trans. 2* **2000**, 2453. (b) Setsukinai, K.; Urano, Y.; Kakinuma, K.; Majima, H. J.; Nagano, T. *J. Biol. Chem.* **2003**, *278*, 3170.
(15) Kawai, K.; Ieda, N.; Aizawa, K.; Suzuki, T.; Miyata, N.; Nakagawa, H. *J. Am. Chem. Soc.* **2013**, *135*, 12690.
(16) (a) Heyne, B.; Maurel, V.; Scaiano, J. C. *Org. Biomol. Chem.* **2006**, *4*, 802. (b) Mak, A. M.; Whiteman, M.; Wong, M. W. *J. Phys. Chem. A* **2007**, *111*, 8202.
(17) (a) Hartman, W. W.; Dickey, J. B.; Stampfli, J. G. *Org. Synth.* **1935**, *15*, 8. (b) Sandford, P. A.; Nafziger, A. J.; Jeanes, A. *Anal. Biochem.* **1971**, *42*, 422.
(18) Drabik, G.; Naskalski, J. W. *Acta Biochim. Polym.* **2001**, *48*, 271.
(19) Lavis, L. D.; Raines, R. T. *ACS Chem. Biol.* **2008**, *3*, 142.
(20) Del Maestro, R.; Thaw, H. H.; Björk, J.; Planker, M.; Arfors, K. E. *Acta Physiol. Scand. Suppl.* **1980**, *492*, 43.
(21) (a) Beilke, M. A.; Collins-Lech, C.; Sohnle, P. G. *J. Lab. Clin. Med.* **1987**, *110*, 91. (b) Imaizumi, N.; Kanayama, T.; Oikawa, K. *Analyst* **1995**, *120*, 1983.
(22) Kojima, H.; Nakatsubo, N.; Kikuchi, K.; Kawahara, S.; Kirino, Y.; Nagoshi, H.; Hirata, Y.; Nagano, T. *Anal. Chem.* **1998**, *70*, 2446.
(23) Schildknecht, S.; Pape, R.; Müller, N.; Robotta, M.; Marquardt, A.; Bürkle, A.; Drescher, M.; Leist, M. *J. Biol. Chem.* **2011**, *286*, 4991.
(24) Lim, M. H.; Xu, D.; Lippard, S. J. *Nat. Chem. Biol.* **2006**, *2*, 375.
(25) (a) Vazquez-Torres, A.; Jones-Carson, J.; Mastroeni, P.; Ischiropoulos, H.; Fang, F. C. *J. Exp. Med.* **2000**, *192*, 227. (b) Vazquez-Torres, A.; Xu, Y.; Jones-Carson, J.; Holden, D. W.; Lucia, S. M.; Dinauer, M. C.; Mastroeni, P.; Fang, F. C. *Science* **2000**, *287*, 1655. (c) Bogdan, C. *Nat. Immunol.* **2001**, *2*, 907. (d) Slauch, J. M. *Mol. Microbiol.* **2011**, *80*, 580.
(26) (a) Heusch, P.; Aker, S.; Boengler, K.; Deindl, E.; van de Sand, A.; Klein, K.; Rassaf, T.; Konietzka, I.; Sewell, A.; Menazza, S.; Canton, M.; Heusch, G.; Di Lisa, F.; Schulz, R. *Am. J. Physiol. Heart Circ. Physiol.* **2010**, *299*, H446. (b) Zhang, W.; Han, Y.; Meng, G.; Bai, W.; Xie, L.; Lu, H.; Shao, Y.; Wei, L.; Pan, S.; Zhou, S.; Chen, Q.; Ferro, A.; Ji, Y. *J. Am. Heart Assoc.* **2014**, *3*, No. e000606.
(27) (a) White, C. R.; Brock, T. A.; Chang, L. Y.; Crapo, J.; Briscoe, P.; Ku, D.; Bradley, W. A.; Gianturco, S. H.; Gore, J.; Freeman, B. A. *Proc. Natl. Acad. Sci. U.S.A.* **1994**, *91*, 1044. (b) Adachi, T.; Weisbrod, R. M.; Pimentel, D. R.; Ying, J.; Sharov, V. S.; Schoneich, C.; Cohen, R. A. *Nat. Med.* **2004**, *10*, 1200.